Energy Efficiency Optimization With Interference Alignment in Multi-Cell MIMO Interfering Broadcast Channels

Jie Tang, *Member, IEEE*, Daniel K. C. So, *Senior Member, IEEE*, Emad Alsusa, *Senior Member, IEEE*, Khairi Ashour Hamdi, *Senior Member, IEEE*, and Arman Shojaeifard, *Member, IEEE*

***Abstract*—Characterizing the fundamental energy efficiency (EE) performance of multiple-input–multiple-output interfering broadcast channels (MIMO-IFBC) is important for the design of green wireless system. In this paper, we propose a new network architecture proposition based on EE maximization for Multi-Cell MIMO-IFBC within the context of interference alignment (IA). Particularly, EE is maximized subject to maximum power and minimum throughput constraints. We propose two schemes to optimize EE for different signal-to-noise ratio (SNR) regions. For high-SNR operating regions, we employ a grouping-based IA scheme to jointly cancel intra- and inter-cell interferences and thus transform the MIMO-IFBC to a single-cell MIMO scenario. A gradient-based power adaptation scheme is proposed based on water-filling power adaptation and singular value decomposition to maximize EE for each cell. For moderate SNR cases, we propose an approach using dirty paper coding (DPC) with the principle of multiple access channel and broadcast channel duality to perform IA while maximizing EE in each cell. The algorithm in its dual form is solved using a subgradient method and a bisection searching scheme. Simulation results demonstrate the superior performance of the proposed schemes over several existing approaches. It also shows that interference-nulling-based IA approaches outperform hybrid DPC-IA approach in high-SNR region, and the opposite occurs in low-SNR region.**

***Index Terms*—Green radio (GR), energy efficiency (EE), multiple input multiple output (MIMO).**

I. Introduction

DENSE deployment of base stations (BSs) with multiple antennas is considered a de facto solution for supporting the projected massive data traffic growth. This trend constitutes to ever-rising network power consumption which has severe implications in terms of both operational and environmental costs. Mobile operators are consequently encompassed with the difficult but fascinating challenge of improving spectral efficiency (SE) and energy efficiency (EE) of network infrastructure at the same time.

Traditionally, SE has been the sole performance indicator for the design of wireless communication networks. It is an important measure for quantifying the effectiveness of cellular systems and has been extensively studied for various technologies and scenarios [1]–[3]. Although SE measures how efficiently a limited frequency spectrum is utilized, it fails to account for energy efficiency. Because of the high power consumption of wireless access networks, research on EE, which is typically concerned with maximizing the total number of bits per Joule, has attracted much interest recently, e.g., single link optimization [4], [5], single-cell scenario [6]–[8], multi-cell deployment [9], [10], cognitive radio [11], [12] and cooperative relaying system [13].

A prominent transmission technology for the next generation of cellular networks such as long-term-evolution advanced (LTE-A) is multiuser (MU) multiple-input multiple-output (MIMO) which facilitates multiplexing data streams across multiple users. In this way, MU-MIMO turns the fundamental problem of single user (SU)-MIMO, i.e., multiplexing data streams for a SU, with low-rank channels into an advantage [14]. Furthermore, in contrast to a SU-MIMO system, scheduling the appropriate set of users based on criteria such as inter-user beamforming correlation factors can lead to additional gains if more transmit antennas are used at the BS [14]. Therefore, adopting MU-MIMO technology can lead to significant improvements in terms of average rate performance. The information-theoretic capacity limit of MIMO broadcast channels (BC) has been extensively studied in the existing literature, e.g., [15]–[17]. In contrast to existing works on capacity or SE of single-cell MIMO-BC that only needs to consider transmit power constraints, studying the EE of single-cell MIMO-BC requires a comprehensive understanding of the power consumption of downlink MU-MIMO systems. In [18], the tradeoff between EE and SE is further exploited by balancing consumption power and occupied bandwidth using resource efficiency for downlink cellular network. In [19], the EE of a scheduler in a single-cell broadcast channel with a random opportunistic beamforming algorithm is investigated. Considering rate balancing constraints for fairness between users, a framework to find the globally optimal energy-efficient solution is proposed in [20]. In [21], a novel optimization approach with antenna selection is developed for improving EE.

On the other hand, SE in multi-cell MU downlink has been well studied in [22]–[25]. The fundamental challenge for

Manuscript received April 11, 2015; accepted May 30, 2015. Date of publication June 5, 2015; date of current version July 13, 2015. This paper was presented in part at the IEEE Global Communications Conference (GLOBECOM) 2014, Austin, TX, USA, 2014. This work was supported by the Engineering and Physical Sciences Research Council of the U.K. under Grant EP/J021768/1. The associate editor coordinating the review of this paper and approving it for publication was R. Schober.

The authors are with the School of Electrical and Electronic Engineering, The University of Manchester, Manchester M13 9PL, U.K. (e-mail: jie.tang@manchester.ac.uk; d.so@manchester.ac.uk; e.alsusa@manchester.ac.uk; k.hamdi@manchester.ac.uk; a.shojaeifard@manchester.ac.uk).

Color versions of one or more of the figures in this paper are available online at http://ieeexplore.ieee.org.

Digital Object Identifier 10.1109/TCOMM.2015.2442246

multi-cell scenario is the mitigation of inter- and intra-cell interferences. Random beamforming (RBF) is a practically favorable transmission scheme for multiuser multi-antenna downlink systems, and a closed-form expression of the achievable average sum-rate in a MISO system is presented in [23]. Considering multiple antennas at the mobile stations, a capacity-maximizing zero-forcing (ZF) scheme for two mutually interfering broadcast channels (IFBC) is proposed in [24]. Furthermore, the authors in [25] proposed a grouping based interference alignment (IA) technique for a network with multi-user MIMO under a Gaussian IFBC scenario with multiple BSs. Compared to the ZF scheme in multi-cell scenario, the grouping based IA scheme requires fewer transmit antennas at the BS. Hence if the same number of antennas is used, the grouping-based approach will have extra spatial dimension than the ZF scheme, which will result in diversity gain. On the other hand, research on EE in IFBC scenario has attracted some interest recently. An energy efficient transmission strategy for multi-cell MU-MISO downlink system by jointly optimizing the transmit powers and beamforming vectors was studied in [10]. However there is a general lack of research study on the EE aspect of multi-cell MU-MIMO system, which is a very practical scenario. There is only [26] which extended the energy efficient optimization problem to a partial-cooperative multi-cell MU-MIMO system by employing the interference zero-forcing (I-ZF) technique.

A. Main Contributions

In this paper, a new network architecture based on EE maximization for multi-cell MIMO-IFBC using IA is proposed. Although IA generally works better in high signal-to-noise ratio (SNR) region, its ability to completely remove inter- and intra-cell interferences is particularly useful in enhancing the SINR, and hence the EE. We propose two schemes to optimize EE in different SNR regions. For high SNR region, we invoke the grouping-based IA scheme from our previous work in [25] to transform the MIMO-IFBC to a single-cell single-user MIMO scenario. We first prove the quasiconcavity of EE based on a fixed transmission power. Then a gradient-based power adaptation scheme is proposed based on water-filling and SVD to maximize EE of each cell. For moderate SNR-range, we propose an approach using DPC and the principle of MAC-BC duality to perform IA while maximizing EE in each cell. A two-layer resource allocation algorithm is then proposed to solve the comprehensive problem based on the fundamental EE to transmission power relationship. A key contribution of this method lies in the inner-layer algorithm which is solved by applying the principle of MAC-BC duality. Particularly, we transform the MIMO-BC problem to the dual MIMO-MAC problem, and based on Lagrange duality and Karush-Kuhn-Tucker (KKT) conditions, we propose a bisection searching algorithm to solve the dual MIMO-MAC problem. Simulation results confirm the validity of our theoretical findings and is further discussed in the results section.

B. Organization and Notation

The remainder of this paper is organized as follows. The system model and problem formulation is given in Section II. In Section III, we briefly revisit the IA scheme based on grouping method for multi-cell MIMO-IFBC. In Section IV, a gradient-based power adaptation scheme is proposed. In Section V, an approach using DPC and the principle of MAC-BC duality has been proposed to perform IA while maximizing EE. Simulation results are provided in Section VI and conclusions are drawn in Section VII.

The following notations are used in the paper. Bold upper and lower case letters denote matrices and vectors, respectively; $(\cdot)^{-1}$ denotes the matrix inverse, $(\cdot)^T$ denotes the matrix transpose, $(\cdot)^H$ denote the matrix conjugate transpose, $\mathbf{I}_{N_t \times N_t}$ denotes an $N_t \times N_t$ identity matrix; $E[\cdot]$ denotes the expectation operator; $\mathrm{Tr}(\cdot)$ denotes the trace of a matrix, $[x]^+$ denotes $\max(x, 0)$; $\mathrm{span}(\cdot)$ indicates the subspace spanned by the column vectors of a matrix; $(\cdot)^b$ and $(\cdot)^m$ denote the quantities associated with a broadcast channel and a multiple access channel, respectively.

II. System Model and Problem Formulation

In this section, we introduce the system model of MIMO-IFBC and formulate the EE optimization problem.

A. System Model

Consider a downlink cellular system with multiple cells (L) and each cell serves K multiple users with N_t transmit and N_r receive antennas, corresponds to a MIMO-IFBC scenario (see Fig. 1). The information transmitted from each BS to any of its respective users consists of d_s data streams where $d_s \leq \min(N_t, N_r) = N_r$. In the l^{th} cell, the intended signal from the serving BS to the k^{th} user is expressed as

$$\mathbf{x}_{[k,l]} = \sum_{i=1}^{d_s} \mathbf{v}^i_{[k,l]} s^i_{[k,l]} = \mathbf{V}_{[k,l]} \mathbf{s}_{[k,l]}, \tag{1}$$

where $s^i_{[k,l]}$ is the i^{th} data symbol transmitted to the k^{th} user in the l^{th} cell, under an average power constraint, $E[\|\mathbf{x}_{[k,l]}\|^2] \leq P_{[k,l]}$, and $\mathbf{v}^i_{[k,l]} \in C^{N_t \times 1}$ is the linear transmit beamforming vector corresponding to $s^i_{[k,l]}$ with a unity norm constraint $\|\mathbf{v}^i_{[k,l]}\| = 1$. The transmitter beamforming matrix for user $[k, l]$ is written as $\mathbf{V}_{[k,l]} = \left[\mathbf{v}^1_{[k,l]}\ \mathbf{v}^2_{[k,l]}\ \cdots\ \mathbf{v}^{d_s}_{[k,l]}\right] \in C^{N_t \times d_s}$, and its corresponding data signal vector is denoted by $\mathbf{s}_{[k,l]} = \left[s^1_{[k,l]}\ s^2_{[k,l]}\ \cdots\ s^{d_s}_{[k,l]}\right]^T \in C^{d_s \times 1}$. Therefore the received signal at the k^{th} user in the l^{th} cell $\mathbf{y}_{[k,l]} \in C^{N_r \times 1}$ can be formulated as

$$\begin{aligned}
\mathbf{y}_{[k,l]} &= \sum_{i=1}^{L} \mathbf{H}^i_{[k,l]} \sum_{j=1}^{K} \mathbf{x}_{[j,i]} + \mathbf{n}_{[k,l]} \\
&= \underbrace{\mathbf{H}^l_{[k,l]} \mathbf{V}_{[k,l]} \mathbf{s}_{[k,l]}}_{\text{desired signal}} + \underbrace{\sum_{j=1, j\neq k}^{K} \mathbf{H}^l_{[k,l]} \mathbf{V}_{[j,l]} \mathbf{s}_{[j,l]}}_{\text{inter-user interference}} \\
&\quad + \underbrace{\sum_{i=1, i\neq l}^{L} \sum_{j=1}^{K} \mathbf{H}^i_{[k,l]} \mathbf{V}_{[j,i]} \mathbf{s}_{[j,i]}}_{\text{inter-cell interference}} + \mathbf{n}_{[k,l]},
\end{aligned} \tag{2}$$

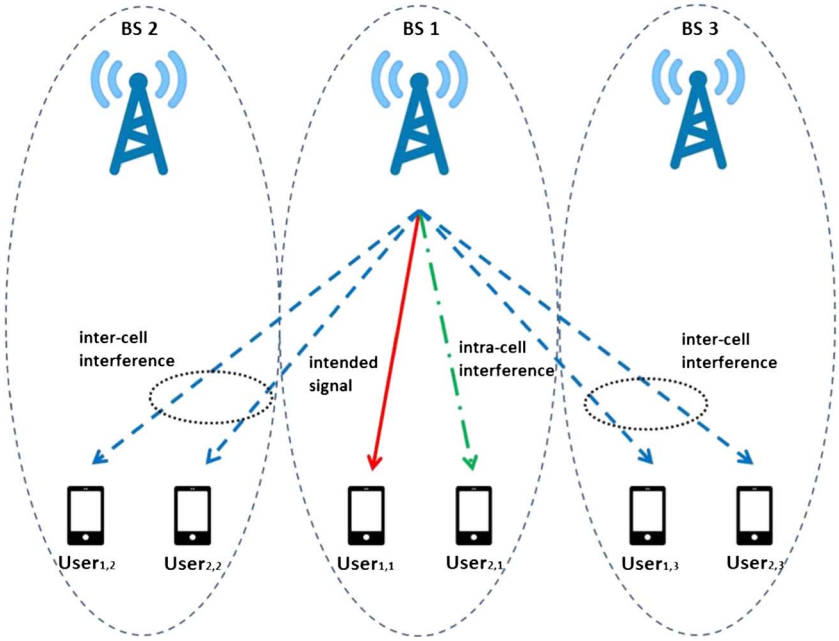

Fig. 1. A multi-cell IA scheme shown for the case of three cells and two users in each cell. In this example, BS 1 tries to convey data information to user 1 while introducing interference to other two cells.

where $\mathbf{n}_{[k,l]} \in C^{N_r \times 1}$ is the additive white Gaussian noise (AWGN) vector with variance σ^2 per entry, and $\mathbf{H}^i_{[k,l]}$ is the $N_r \times N_t$ channel matrix from BS i to user $[k, l]$. The channels are assumed to be independent and identically distributed (i.i.d.) complex Gaussian random variables, i.e., $\mathbf{H}^i_{[k,l]} \sim \mathcal{CN}(0, 1)$. Each channel is further assumed to be quasi-stationary and frequency flat. We also suppose that perfect channel state information (CSI) is available at all BSs and users. This can be achieved where all BSs might share their CSI and data through backhaul links, which enable coordinated transmission for interference management. For the local network, CSI at the receivers (CSIR) can be obtained from the channel estimation of the downlink pilots. CSI at the transmitters (CSIT) can be acquired through uplink feedback in frequency division duplex (FDD) systems or through uplink channel estimation in time division duplex (TDD) systems. The received signal for each user is multiplied by a receiver beamforming matrix to obtain the desired signal from its corresponding BS. The received signal at user $[k, l]$ after the receiver beamformer is given by

$$\begin{aligned}\tilde{\mathbf{y}}_{[k,l]} &= \mathbf{U}^H_{[k,l]}\mathbf{y}_{[k,l]} = \mathbf{U}^H_{[k,l]}\mathbf{H}^l_{[k,l]}\mathbf{V}_{[k,l]}\mathbf{s}_{[k,l]} \\ &\quad + \mathbf{U}^H_{[k,l]}\left(\sum_{j=1,j\neq k}^{K}\mathbf{H}^l_{[k,l]}\mathbf{V}_{[j,l]}\mathbf{s}_{[j,l]}\right. \\ &\quad \left. + \sum_{i=1,i\neq l}^{L}\sum_{j=1}^{K}\mathbf{H}^i_{[k,l]}\mathbf{V}_{[j,i]}\mathbf{s}_{[j,i]}\right) + \tilde{\mathbf{n}}_{[k,l]}, \qquad (3)\end{aligned}$$

where $\mathbf{U}_{[k,l]} = [\mathbf{u}^1_{[k,l]}\ \mathbf{u}^2_{[k,l]}\ \cdots\ \mathbf{u}^{d_s}_{[k,l]}] \in C^{N_r \times d_s}$ denotes the receiver beamforming matrix for this user, and $\tilde{\mathbf{n}}_{[k,l]} = \mathbf{U}^H_{[k,l]}\mathbf{n}_{[k,l]}$ is the effective noise component at the output of the beamformer which is distributed according to $\mathcal{CN}(0, 1)$ given that the receiver beamforming matrix $U_{[k,l]}$ is unitary.

It is well-known that BSs are the primary source of energy consumption in cellular networks. Due to the recent advances in circuit technology, it has been made possible for wireless transceivers to consume different power levels in different operational modes. These include BS sleep, idle, transmit, and receive modes which can be accordingly adjusted based on the daily fluctuations in network load for the purpose of saving energy [27]. Defining a quantitative BS power model is nevertheless challenging given one needs to take into consideration the particular deployment scenario and components configurations. The following linear power model is however shown to be a reasonable approximation [28]

$$P = \zeta P_T + P_c \qquad (4)$$

where ζ, P_T and P_c are respectively used to denote the reciprocal of drain efficiency of the power amplifier, transmission power, and circuit power consumption which can be divided into static and dynamic parts that depend on the parameters of the active links. In this paper, the dynamic part is modeled as a linear function of the number of active antennas [29]

$$P_c = P_s + P_{ant}N_t \qquad (5)$$

where P_s is the static circuit power in transmit mode, $P_{ant}N_t$ denotes the dynamic power consumption proportional to the number of active transmit antennas. It is noted that dynamic antenna selection approach in the single cell system [21] is not included in this work and hence fixed antenna strategy is employed in our multi-cell scenario. It should also be noted that the signal processing power running the proposed algorithms is not included in the BS power model under consideration. This is based on the realistic assumption that P_c is significantly greater than the power required for practical implementation of the corresponding algorithms.

B. Problem Formulation

Conventional EE for downlink transmission is defined as the total number of delivered bits per unit energy, where energy consumption includes transmission energy consumption and circuit energy consumption in active mode. Hence, we define EE of the l^{th} cell in MIMO-IFBC as

$$\lambda_{EE}^{[l]} \triangleq \frac{C_{BC}^{[l]}}{P} = \frac{\sum_{k=1}^{K} C_{[k,l]}}{\zeta P_T^{[l]} + P_c}, \tag{6}$$

where $C_{[k,l]}$ is the capacity achieved by the k^{th} user in the l^{th} cell and $P_T^{[l]}$ is the total transmission power for BS l. The objective of this paper is to maximize the EE of each cell in MIMO-IFBC whilst achieving a desirable throughput. It is therefore reasonable to maximize EE subject to satisfying a minimum throughput requirement. Based on the total power consumption mode in (4) and noting that $P_T^{[l]} = \sum_{k=1}^{K} P_{[k,l]}$, the optimization problem for cell l can be formulated as

$$\max \ \lambda_{EE}^{[l]} \tag{7}$$

$$\text{s.t.} \quad \sum_{k=1}^{K} P_{[k,l]} \le P_{max}^{[l]}, \tag{8}$$

$$\sum_{k=1}^{K} C_{[k,l]} \ge \delta_{\min}^{[l]}, \tag{9}$$

where $P_{max}^{[l]}$ and $\delta_{\min}^{[l]}$ are the maximum total transmit power constraint at BS l and minimum throughput constraint for cell $l \in (1, 2, \cdots, L)$, respectively. Due to the existence of inter-channel interference and intra-cell interference in MIMO-IFBC, the solution of the above problem is nontrivial and cannot be solved directly. Therefore, in the following sections, we develop resource allocation schemes for IA based systems to solve the above optimization problem.

III. Interference Alignment in Multi-Cell MIMO-IFBC

In this section, we design interference mitigation techniques in order to jointly remove the intra- and inter-cell interferences. Zero-forcing (or null-steering) precoding is a method of spatial signal processing by which the multiple antenna transmitter can null multiuser interference signals in wireless communications. Therefore, to remove both intra- and inter-cell interferences, we need to apply the ZF scheme which requires $N_t = (K \times L) \times d_s$ transmit antennas [26]. On the other hand, grouping-based IA solution [25] is capable of removing both the intra- and inter-cell interferences but with fewer transmit antennas at each BS, i.e., $N_t = [K(L-1)+1] \times d_s$, and hence we can exploit the unused spatial dimension to provide extra diversity gain compared to the ZF approach. As a result, we employ the grouping-based IA solution from [25] in this work. The key steps of this approach is revisited here for completeness of this paper. The IA scheme under consideration group users to a subspace and then designs the receiver beamforming matrices. Once the effective inter- and intra-cell interfering channels are identified, we design the transmit beamforming matrices.

Step 1—Receiver Beamforming Design Using Grouping Method: In the first step, we group users into a certain interference space. We consider the users $[1, l+1], \cdots, [K, l+1]$ in the $(l+1)^{th}$ cell as an example. Without loss of generality, in order to align the inter-cell interfering channels from the l^{th} BS to the same subspace, users in the $(l+1)^{th}$ cell are grouped together using the receiver beamforming matrices $\mathbf{U}_{[1,l+1]}, \cdots, \mathbf{U}_{[K,l+1]}$ as (10), shown at the bottom of the page. To find the intersection subspace $\mathbf{F}_l$ and the corresponding receiver beamforming matrices, we solve the matrix equation as in (11), shown at the bottom of the page. As a result, all users in the l^{th} cell are grouped together and the interference to users in each group can be treated as interference to one destination.

Step 2—Designing the Transmit Beamforming Matrices: Using the grouping method in step 1, the effective inter-cell interference channels are mutually aligned and hence the l^{th} BS can treat the K different inter-cell interference channel vectors as a single inter-cell interference channel vector which spans the d_s dimensional subspace as shown in (10). Hence, we design the transmit beamforming vectors for the k^{th} user in the l^{th} cell $\mathbf{V}^{[k,l]}$ as (12), shown at the bottom of the next page, such that the symbols sent from BS l do not cause interference to users in other cells as well as other users in the same cell. Hence, we can design the transmit and receiver beamforming matrices

$$\mathbf{F}_l = \text{span}\left\{\mathbf{H}_{[1,l+1]}^{lH}\mathbf{U}_{[1,l+1]}\right\} = \text{span}\left\{\mathbf{H}_{[2,l+1]}^{lH}\mathbf{U}_{[2,l+1]}\right\} = \cdots = \text{span}\left\{\mathbf{H}_{[K,l+1]}^{lH}\mathbf{U}_{[K,l+1]}\right\} \tag{10}$$

$$\begin{bmatrix} \mathbf{I}_{N_t} & -\mathbf{H}_{[1,l+1]}^{lH} & \mathbf{0} & \cdots & \mathbf{0} \\ \mathbf{I}_{N_t} & \mathbf{0} & -\mathbf{H}_{[2,l+1]}^{lH} & \cdots & \mathbf{0} \\ \vdots & \vdots & \vdots & \ddots & \vdots \\ \mathbf{I}_{N_t} & \mathbf{0} & \mathbf{0} & \cdots & -\mathbf{H}_{[K,l+1]}^{lH} \end{bmatrix} \begin{bmatrix} \mathbf{F}_l \\ \mathbf{U}_{[1,l+1]} \\ \mathbf{U}_{[2,l+1]} \\ \vdots \\ \mathbf{U}_{[K,l+1]} \end{bmatrix} = \mathbf{F}_l\mathbf{X}_l = \mathbf{0} \tag{11}$$

for all users using this two-step scheme. Following these two steps, the required minimum number of transmit antennas N_t is $[K(L-1)+1]\times d_s$, while the required minimum number of receive antennas N_r is $[(K-1)(L-1)+1]\times d_s$.

It should be note that if we design the receiver beamformers in a different way such that all other users are grouped together (i.e., those outside the l^{th} cell), a lower number of transmit antennas is required for BS l. On the hand, all other BSs would need more transmit antennas in order to perform perfect interference alignment given that the users' receiver beamformers are already designed. This approach therefore leads to a higher computational complexity than the proposed grouping method.

IV. Energy Efficiency in Multi-Cell MIMO-IFBC With Interference Alignment

The IA scheme using the grouping method in Section III can ensure zero intra- and inter-cell interference at the receiver of each user. Considering the k^{th} user in the l^{th} BS, the effective channel after applying IA is

$$\tilde{\mathbf{H}}^{l}_{[k,l]} = \mathbf{U}^{H}_{[k,l]}\mathbf{H}^{l}_{[k,l]}\mathbf{V}_{[k,l]}, \tag{13}$$

and $\tilde{\mathbf{H}}^{l}_{[k,l]} \in C^{d_s\times d_s}$. Since there does not exist any intra- and inter-cell interference, the multiple-cells with multiple MIMO users scenario has been transformed to a single-cell single user MIMO case. SVD precoding is known to achieve the MIMO channel capacity since the transmitter emits multiple streams in the eigen-directions of the channel covariance matrix. The SVD of the effective channel $\tilde{\mathbf{H}}^{l}_{[k,l]}$ is given by

$$\tilde{\mathbf{H}}^{l}_{[k,l]} = \mathbf{U}^{s}_{[k,l]}\mathbf{\Sigma}^{l}_{[k,l]}\mathbf{V}^{sH}_{[k,l]}, \tag{14}$$

where $\mathbf{U}^{s}_{[k,l]}$ is a $d_s\times d_s$ unitary matrix which contains the left-singular vectors, $\mathbf{V}^{s}_{[k,l]}$ is a $d_s\times d_s$ unitary matrix which contains the right-singular vectors and $\mathbf{\Sigma}^{l}_{[k,l]}$ is a diagonal matrix having entries as the singular values of $\tilde{\mathbf{H}}^{l}_{[k,l]}$. Hence, the overall transmit beamforming matrix for this user is written as

$$\tilde{\mathbf{V}}_{[k,l]} = \mathbf{V}_{[k,l]}\mathbf{V}^{s}_{[k,l]}, \tag{15}$$

where $\mathbf{V}_{[k,l]}$ ensures IA to cancel both inter- and intra-cell interference, and $\mathbf{V}^{s}_{[k,l]}$ is a matrix that contains the right-singular vectors of the effective channel $\tilde{\mathbf{H}}^{l}_{[k,l]}$. Similarly, the receive beamformer matrix is written as

$$\tilde{\mathbf{U}}_{[k,l]} = \mathbf{U}_{[k,l]}\mathbf{U}^{s}_{[k,l]}, \tag{16}$$

where $\mathbf{U}_{[k,l]}$ ensures users are grouped to a particular interference space and $\mathbf{U}^{s}_{[k,l]}$ is a matrix that contains the right-singular vectors of the effective channel $\tilde{\mathbf{H}}^{l}_{[k,l]}$. After applying IA and SVD, the rate achieved by this user is

$$r_{[k,l]} = \sum_{i=1}^{d_s} B\log_2\left(1+p^{l}_{[k,i]}g^{l}_{[k,i]}\right) \tag{17}$$

where B represents the transmission bandwidth, $p^{l}_{[k,i]}$ denotes the power allocated on the i^{th} data stream of the k^{th} user, $g^{l}_{[k,i]} = \frac{\gamma^{l}_{[k,i]}}{\sigma^2}$ denotes the effective channel-gain-to-noise ratio of user $[k,l]$ for the i^{th} data stream and $\gamma^{l}_{[k,i]}$ is the i^{th} singular value of the effective channel $\tilde{\mathbf{H}}^{l}_{[k,l]}$. Since there does not exist any inter-cell interference, the multi-cell scenario has been transformed into a single-cell scenario and the cell index l can been removed, i.e., $r_{[k,l]}$ is changed to r_k. Therefore, the original optimization problem in (7)–(9) has now been transferred to the following problem

$$\max_{p_{[k,i]}\geq 0} \frac{\sum_{k=1}^{K} r_k}{\zeta\sum_{k=1}^{K}\sum_{i=1}^{d_s} p_{[k,i]} + P_c} \tag{18}$$

$$\text{s.t.} \quad \sum_{k=1}^{K}\sum_{i=1}^{d_s} p_{[k,i]} \leq P_{max}, \tag{19}$$

$$\sum_{k=1}^{K} r_k \geq \delta_{\min}, \tag{20}$$

where P_{max} and $\delta_{\min}$ represent the maximum total transmit power for the base station and the minimum cell throughput requirement, respectively.

The problem in (18)–(20) is non-convex and hence is difficult to solve directly. To obtain an insight into the problem, we investigate the properties of the optimization problem which are summarized in the following theorem.

Theorem I: The maximum achievable EE at a certain total transmit power, P_T, is achieved with transmit power $p_{[k,i]}\geq 0$, $\forall\, k\in\mathcal{K}$, $\forall\, i\in\mathcal{S}_i$, that satisfy the constraints in (19), (20), namely,

$$\tilde{\lambda}_{EE}(P_T) \triangleq \max_{p_{[k,i]}\geq 0} \frac{\sum_{k=1}^{K} r_k}{\zeta\sum_{k=1}^{K}\sum_{i=1}^{d_s} p_{[k,i]} + P_c} \tag{21}$$

$$\mathbf{V}_{[k,l]} \subset \text{null}\left(\left[\underbrace{\mathbf{F}_l}_{\substack{\text{effective}\\ \text{interference channels}}} \underbrace{\left(\mathbf{U}^{H}_{[t(t=1,\cdots,K),s(s\neq l,l+1)]}\mathbf{H}^{lH}_{[t(t=1,\cdots,K),s(s\neq l,l+1)]}\right)}_{\substack{\text{effective}\\ \text{inter-cell interference channel}}} \underbrace{\left(\mathbf{U}^{H}_{[t(t\neq k),l]}\mathbf{H}^{lH}_{[t(t\neq k),l]}\right)}_{\substack{\text{effective}\\ \text{intra-cell interference channel}}}\right]^{H}\right) \tag{12}$$

subject to

$$\sum_{k=1}^{K}\sum_{i=1}^{d_s} p_{[k,i]} = P_T, \tag{22}$$

$$\sum_{k=1}^{K} r_k \geq \delta_{\min}, \tag{23}$$

has the following properties:

(i) $\tilde{\lambda}_{EE}(P_T)$ is continuously differentiable and quasiconcave in P_T,
(ii) The derivative of EE satisfies

$$\frac{d\tilde{\lambda}_{EE}(P_T)}{dP_T} = \frac{\frac{d\tilde{R}(P_T)}{P_T} - \zeta\tilde{\lambda}_{EE}(P_T)}{\zeta P_T + P_C} \tag{24}$$

where

$$\tilde{R}(P_T) \triangleq \max_{p_{[k,i]}\geq 0} R(P_T) = \max_{p_{[k,i]}\geq 0}\sum_{k=1}^{K} r_k \tag{25}$$

is the maximum sum-rate under constraints (22), (23), and its derivative satisfies

$$\frac{d\tilde{R}(P_T)}{P_T} = \max_{k\in\mathcal{K}, i\in\mathcal{S}_i} \frac{Wg_{[k,i]}\log_2 e}{1+\tilde{p}_{[k,i]}g_{[k,i]}} \tag{26}$$

where $\tilde{p}_{[k,i]}$ is the optimal power on the i^{th} data streams of k^{th} users for achieving $\tilde{R}(P_T)$.

Proof: See Appendix A.

Our next step is to find out the optimal power allocation scheme to maximize sum-rate. Similar to [7], the optimal power can be calculated using the following water-filling scheme

$$\bar{p}_{[k,i]} = \left(\mu_s - \frac{1}{g_{[k,i]}}\right)^+, \tag{27}$$

$$\sum_{k\in\mathcal{K}}\sum_{i\in\mathcal{S}_i} W\log_2\left(\mu_s g_{[k,i]}\right) = \delta_{\min}, \tag{28}$$

$$\tilde{p}_{[k,i]} = \bar{p}_{[k,i]} + \left(\mu - \frac{1}{g_{[k,i]}} - \bar{p}_{[k,i]}\right)^+, \tag{29}$$

$$\sum_{k\in\mathcal{K}}\sum_{i\in\mathcal{S}_i}\left(\mu - \frac{1}{g_{[k,i]}} - \bar{p}_{[k,i]}\right) = P_T - \sum_{k\in\mathcal{K}}\sum_{i\in\mathcal{S}_i}\bar{p}_{[k,i]}, \tag{30}$$

where μ_s and μ are intermediate variables. The idea of the water-filling process includes two steps. We first allocate power using (27), (28) to satisfy the minimum rate requirement. The total power used in the first step is $P_0 = \sum_{k\in\mathcal{K}}\sum_{i\in\mathcal{S}_i}\bar{p}_{[k,i]}$. It must be noted that if the power used to satisfy the minimum rate requirement is larger than the power budget, i.e., $P_0 > P_{max}$, the EE optimization problem in (21), (23) is infeasible. We then allocate the remaining power $(P_T - P_0)$ using (29), (30) to further maximize the sum rate. This scheme can be straightforwardly implemented by the approach of Lagrange multiplier and the derivations of (27)–(30).

TABLE I
GRADIENT-BASED OPTIMAL POWER ADAPTATION SCHEME

1) Do single-user water-filling using (27)-(28) to get $\bar{p}_{k,n}$ and μ_s, calculate the power consumption P_0;
2) **IF** $P_0 > P_{max}$
3) infeasible;
4) **ELSE**
5) Initial Power $P_T(0) \in [P_0, P_{max}]$;
6) **REPEAT**
7) For the remaining power, do the water-filling in (29)-(30);
8) Update transmission power using gradient of EE as in (31);
9) **STOP** when $|P_T(n) - P_T(n-1)| \leq \varepsilon$.
10) **END**

Since there exists a unique optimal point for any quasiconcave function, Property (i) in *Theorem I* guarantees the existence and uniqueness of the maximum and indicates the differentiability of $\tilde{\lambda}_{EE}(P_T)$. Moreover, due to the property of quasiconcavity, $\tilde{\lambda}_{EE}(P_T)$ either strictly decreases or first increases and then strictly decreases with P_T starting from P_0. Property (ii) further reveals that the optimal point is guaranteed at a finite transmit power. Consequently, we can combine a derivative-assisted gradient scheme and water-filling approach in (27)–(30) to obtain the optimal solution for (18)–(20). We call this algorithm as gradient-based power adaptation approach. Particularly, we update the transmission power as

$$P_T(n) = P_T(n-1) + t\times\frac{d\tilde{\lambda}_{EE}(P_T)}{dP_T}, \tag{31}$$

where t is a small step size. For the updated transmission power, P_T, we apply the multi-level water-filling approach in (27)–(30) again to obtained the optimal power allocation. This process is repeated until ε-optimality reached, i.e., $|P_T(n) - P_T(n-1)| \leq \varepsilon$. It is noted that the gradient-based power adaptation method will end with P_0 if $\tilde{\lambda}_{EE}(P_T)$ is monotonically decreasing in $[P_0, P_{max}]$ and P_{max} if $\tilde{\lambda}_{EE}(P_T)$ is monotonically increasing in $[P_0, P_{max}]$. The gradient-based optimal power adaptation scheme is detailed in Table I.

V. ENERGY EFFICIENCY IN MULTI-CELL MIMO-IFBC WITH HYBRID INTERFERENCE ALIGNMENT

The IA scheme presented in Section III fully utilizes the available degrees of freedom for transmission. The grouping-based IA method is therefore best suited, and in fact capacity-optimal, in high SNR operating regimes. On the other hand, pure IA may lead to lower network capacity in low to intermediate SNR region due to the lack of coherent array gain [30]. Hence, we propose a hybrid approach by applying IA only for the inter-cell users and tackle the intra-cell interference among users by using DPC, which is a capacity-achieving scheme for MIMO-BC, to maximize EE of each cell.

A. Hybrid IA Scheme With Dirty Paper Coding

The first step of the hybrid scheme involves a classical IA approach with the beamformer matrix for the k^{th} user in the l^{th} cell written as

$$\bar{\mathbf{V}}_{[k,l]} = \mathbf{V}_l\mathbf{W}_{[k,l]}, \tag{32}$$

where $\mathbf{V}_l$ ensures inter-cell interference is removed, and $\mathbf{W}_{[k,l]}$ is a matrix that optimally combines the column space of $\mathbf{V}_l$ towards maximizing the intra-cell EE. Therefore, $\bar{\mathbf{V}}_{[k,l]}$ is the hybrid transmit beamforming matrix for user $[k,l]$ which is aimed at removing inter-cell interference while maximizing EE of cell l. Furthermore, the IA subspace $\mathbf{V}_l$ in this case should be modified as (33), shown at the bottom of the page, where $\mathbf{V}_l$ represents the base spaces in the BS l. Once the IA subspace $\mathbf{V}_l$ is determined using (33), we then proceed by finding the optimal combination matrices to maximize EE. Hence, the original problem is now concerned with designing the optimal weight vector $\mathbf{W}_{[k,l]}$, which is solved by using DPC. Without loss of generality, we assume the encoding order is $(1, 2, \cdots, K)$, i.e., the codeword of user 1 is encoded first. The data rate $R^b_{[k,l]}$ for the k^{th} user in the l^{th} cell is written as [31]

$$R^b_{[k,l]} = \log \frac{\left|\mathbf{I} + \sum_{i=k}^{K} \bar{\mathbf{H}}^l_{[i,l]} \mathbf{Q}^b_{[i,l]} \bar{\mathbf{H}}^{lH}_{[i,l]}\right|}{\left|\mathbf{I} + \sum_{i=k+1}^{K} \bar{\mathbf{H}}^l_{[i,l]} \mathbf{Q}^b_{[i,l]} \bar{\mathbf{H}}^{lH}_{[i,l]}\right|}, \tag{34}$$

where $\bar{\mathbf{H}}^l_{[k,l]}$ represents the effective channel from BS l to its k^{th} user which is given by

$$\bar{\mathbf{H}}^l_{[k,l]} = \mathbf{U}^H_{[k,l]} \mathbf{H}^l_{[k,l]} \mathbf{V}_l, \tag{35}$$

and $\mathbf{Q}^b_{[i,l]} = \{\mathbf{W}_{[i,l]} \mathbf{W}^H_{[i,l]}\}$ represents the virtual transmit covariance matrix for user $[i,l]$, $\mathbf{Q}^b_{[i,l]} \succeq 0$. Similar to the analysis from Section IV, given there exists no inter-cell interference, the multi-cell scenario is transformed into a single-cell scenario and therefore the cell index is removed. Hence, the EE maximization problem in (7)–(9) can be rewritten as

$$\max_{\mathbf{Q}^b_k \succeq 0} \quad \frac{C_{BC}\left(\bar{\mathbf{H}}_1, \cdots, \bar{\mathbf{H}}_K, \mathbf{Q}^b_1, \cdots, \mathbf{Q}^b_K\right)}{\zeta \sum_{k=1}^{K} \mathrm{Tr}\left(\mathbf{Q}^b_k\right) + P_c} \tag{36}$$

$$\text{s.t.} \quad \sum_{k=1}^{K} \mathrm{Tr}\left(\mathbf{Q}^b_k\right) \le P_{max}, \tag{37}$$

$$\sum_{k=1}^{K} R^b_k \ge \delta_{\min}, \tag{38}$$

where $C_{BC}(\bar{\mathbf{H}}_1, \cdots, \bar{\mathbf{H}}_K, \mathbf{Q}^b_1, \cdots, \mathbf{Q}^b_K) = \sum_{k=1}^{K} R^b_k$ and P_{max} denotes the power budget. The optimization problem in (36)–(38) is a EE optimization problem for MIMO-BC. However, this is not a convex problem, and hence it cannot be solved directly. In the following section, we exploit the fundamental property for EE optimization problem and develop a two-layer resource allocation scheme based on MAC-BC duality and bisection searching scheme.

B. Equivalence and Duality

Authors in [31] proved that the capacity region of the MIMO MAC with a total power constraint P for all K transmitters is the same as the dirty paper region of the dual MIMO BC with power constraint P. In other words, any rate vector that is achievable in the dual MAC with power constraints $(P_1, P_2, \cdots, P_K)$ is in the dirty paper region of the BC with power constraint $\sum_{k=1}^{K} P_k$. Conversely, any rate vector that is in the dirty paper region of the BC is also in the dual MIMO MAC region with the same total power constraint. Furthermore, [16] showed the DPC achievable rate region in the Gaussian MIMO BC is in fact the capacity region. Hence, the dirty paper region of a MIMO BC with power constraint P is equal to the capacity region of the dual MIMO MAC with total power constraint P:

$$\mathcal{C}_{DPC}(P, \mathbf{H}) = \mathcal{C}_{BC}(P, \mathbf{H}) = \mathcal{C}_{MAC}(P, \mathbf{H}^H). \tag{39}$$

By exploiting the MAC-BC duality theorem, the optimization problem in (36)–(38) is equivalent to the following problem

$$\max_{\mathbf{Q}^m_k \succeq 0} \quad \frac{C_{MAC}\left(\bar{\mathbf{H}}^H_1, \cdots, \bar{\mathbf{H}}^H_K, \mathbf{Q}^m_1, \cdots, \mathbf{Q}^m_K\right)}{\zeta \sum_{k=1}^{K} \mathrm{Tr}\left(\mathbf{Q}^m_k\right) + P_c} \tag{40}$$

$$\text{s.t.} \quad \sum_{k=1}^{K} \mathrm{Tr}\left(\mathbf{Q}^m_k\right) \le P_{max}, \tag{41}$$

$$\sum_{k=1}^{K} R^m_k \ge \delta_{\min}, \tag{42}$$

where C_{MAC} is the rate of the dual MAC, and $\mathbf{Q}^m_k$ is the transmit covariance matrix of the user k. Here, constraint (41) and (42) is the upper and lower bound for the optimization problem. This problem can be solved using the Dinkelbachs method [32]–[34] in a parameterized concave form by separating the numerator and the denominator with the help of parameter λ. In particular, the concave form of the fractional program is established by denoting the objective function value as λ so that a subtractive form of the objective function may be written as $F(\lambda) = C_{MAC} - \lambda \times (P_T + P_c)$, which is concave. An iterative method is then employed to find increasing λ values that are feasible by solving the parameterized problem of $\max F(\lambda(n))$ at each iteration. Hence, it can be shown that the method produces an increasing sequence of λ values which converges to the optimal value. However, the Dinkelbachs method cannot provide insights on the property of EE in MIMO-BC, i.e., the relationship between EE and transmission power P_T. Thus motivated by the fundamental property for EE in SISO system [27], we develop the following theorems and propose a more efficient two-layer scheme to obtain the maximum EE in a MIMO-BC scenario.

$$\mathbf{V}_l \subset \mathrm{null}\left(\left[\underbrace{\mathbf{G}_l}_{\text{effective interference channels}} \quad \underbrace{\left(\mathbf{U}^H_{[t(t=1,\cdots,K),s(s\neq l,l+1)]} \mathbf{H}^{lH}_{[t(t=1,\cdots,K),s(s\neq l,l+1)]}\right)}_{\text{effective inter-cell interference channel}}\right]^H\right) \tag{33}$$

Theorem II: For any given transmission power P_T, achieved with transmit covariance matrix $\mathbf{Q}_k^m, \forall\, k \in \mathcal{K}$, that satisfy the constraints in (41), (42), the maximum EE, $\lambda_{EE}^* = \max_{\mathbf{Q}_k^m \succeq 0} \lambda_{EE}(P_T)$, is strictly quasiconcave in P_T.

Proof: See Appendix B.

Theorem III: In the transmission power region $[P_{min}, P_{max}]$, the maximum EE, $\lambda_{EE}^*(P_T)$

(i) strictly decreases with P_T and is maximized at $P_T = P_{min}$ if

$$\left.\frac{d\lambda_{EE}^*(P_T)}{dP_T}\right|_{P_T=P_{min}} \leq 0,$$

(ii) strictly increases with P_T and is maximized at $P_T = P_{max}$ if

$$\left.\frac{d\lambda_{EE}^*(P_T)}{dP_T}\right|_{P_T=P_{min}} > 0 \;\text{ and }\; \left.\frac{d\lambda_{EE}^*(P_T)}{dP_T}\right|_{P_T=P_{max}} \geq 0,$$

(iii) first strictly increases and then strictly decreases with P_T and is maximized at $P_T = \frac{C_{MAC}(\lambda_{EE}^{opt})}{\lambda_{EE}^{opt}}$ if

$$\left.\frac{d\lambda_{EE}^*(P_T)}{dP_T}\right|_{P_T=P_{min}} > 0 \;\text{ and }\; \left.\frac{d\lambda_{EE}^*(P_T)}{dP_T}\right|_{P_T=P_{max}} < 0,$$

(iv) infeasible if

$$P_{min} > P_{max},$$

where P_{min} is the minimum transmission power under all constraints in (41), (42) and $C_{MAC}(\lambda_{EE}^{opt})$ is the throughput that corresponds to the maximum EE under all constraints in (41), (42).

Proof: See Appendix C.

Since there exists a unique maximum for any quasiconcave function, *Theorem II* guarantees the existence and uniqueness of a maximum solution. Furthermore, $\lambda_{EE}^*(P_T)$ either strictly decreases or first increases and then strictly decreases with P_T starting from P_{min}, which is the minimum transmission power to satisfy the minimum throughput requirement. *Theorem III* further indicates that the maximum point is always achieved at a finite transmission power. Therefore, the problem in (40)–(42) can be decomposed into two layers and solved iteratively through the following processes.

(i) Inner-layer: For a given transmission power, P_T, finds the maximum EE $\lambda_{EE}^*(P_T)$.
(ii) Outer-layer: Finds the optimal EE, λ_{EE}^{opt}, via a gradient-based algorithm.

The key of the proposed scheme lies in the inner-layer algorithm to find the maximum EE $\lambda_{EE}^*(P_T)$ based on a given transmission power, i.e., any P_T in the power region $[P_{min}, P_{max}]$. Hence, the optimization problem in (40)–(42) can be expressed as

$$\max_{\mathbf{Q}_k^m \succeq 0} \quad \frac{C_{MAC}\left(\bar{\mathbf{H}}_1^H, \cdots, \bar{\mathbf{H}}_K^H, \mathbf{Q}_1^m, \cdots, \mathbf{Q}_K^m\right)}{\zeta \sum_{k=1}^K \mathrm{Tr}\left(\mathbf{Q}_k^m\right) + P_c} \tag{43}$$

$$\text{s.t.} \quad \sum_{k=1}^K \mathrm{Tr}\left(\mathbf{Q}_k^m\right) = P_T, \tag{44}$$

where the capacity region of the dual MIMO-MAC $C_{MAC}(\bar{\mathbf{H}}_1^H, \cdots, \bar{\mathbf{H}}_K^H, \mathbf{Q}_1^m, \cdots, \mathbf{Q}_K^m) = W \log |\mathbf{I}_{N_t \times N_t} + \frac{1}{\sigma^2} \sum_{k=1}^K \mathbf{H}_k^H \mathbf{Q}_k^m \mathbf{H}_k|$. We hereafter refer to this minimization problem as the dual MAC optimization problem. Since the objective function is convex given the constraint is a convex set, the dual MAC optimization problem is a convex problem and can be solved in an efficient manner. Hence, the inner-layer of the proposed algorithm has been transformed to solve the optimization problem in (43), (44) based on a given transmission power P_T. In the next section, we will introduce a method to solve the dual MAC optimization problem under consideration.

C. Dual MAC Optimization Problem

Defining $f(\mathbf{Q}_1^m, \cdots, \mathbf{Q}_K^m) = \log |\mathbf{I}_{N_t \times N_t} + \frac{1}{\sigma^2} \sum_{k=1}^K \mathbf{H}_k^H \mathbf{Q}_k^m \mathbf{H}_k|$, we rewrite the optimization problem in (43), (44) as

$$\max_{\mathbf{Q}_k^m \succeq 0} f\left(\mathbf{Q}_1^m, \cdots, \mathbf{Q}_K^m\right) \quad s.t. \sum_{k=1}^K \mathrm{Tr}\left(\mathbf{Q}_k^m\right) = P_T. \tag{45}$$

Since the positive semi-definiteness of $\mathbf{Q}_k^m$ is equivalent to the non-negativeness of the eigenvalues of $\mathbf{Q}_k^m$, i.e., $q_{k,j} \geq 0$, the Lagrangian function is given by

$$L\left(\mathbf{Q}_1^m, \cdots, \mathbf{Q}_K^m, \eta, \delta_{k,j}\right) := f\left(\mathbf{Q}_1^m, \cdots, \mathbf{Q}_K^m\right) - \eta\left(\sum_{k=1}^K \mathrm{Tr}\left(\mathbf{Q}_k^m\right) - P_T\right) + \sum_{k=1}^K \sum_{j=1}^M \delta_{k,j} q_{k,j}, \tag{46}$$

where $\eta \geq 0$ and $\delta_{k,j} \geq 0$ are the Lagrangian multipliers associated with the maximum power constraint and the positive eigenvalues constraints, respectively. M is the number of positive eigenvalues. In accordance with the KKT conditions of (45), we have

$$\frac{\partial f\left(\mathbf{Q}_1^m, \cdots, \mathbf{Q}_K^m\right)}{\partial \mathbf{Q}_k^m} - \eta \mathbf{I}_{N_r \times N_r} + \sum_{j=1}^M \delta_{k,j} \frac{\partial q_{k,j}}{\partial \mathbf{Q}_k^m} = 0, \tag{47}$$

$$\eta\left(\sum_{k=1}^K \mathrm{Tr}\left(\mathbf{Q}_k^m\right) - P_T\right) = 0, \tag{48}$$

$$\delta_{k,j} q_{k,j} = 0. \tag{49}$$

The dual objective function of the optimization problem in (45) is

$$g(\eta) = \max_{\mathbf{Q}_k^m \succeq 0} L\left(\mathbf{Q}_1^m, \cdots \mathbf{Q}_K^m, \eta\right), \tag{50}$$

and the dual problem is shown as

$$\min g(\eta) \quad s.t. \quad \eta \geq 0. \tag{51}$$

In this work, we use an iterative method to obtain the optimal $\mathbf{Q}_k^m$ for the dual MAC problem. $\mathbf{Q}_k^m$ is updated using the

TABLE II
BISECTION BASED RESOURCE ALLOCATION ALGORITHM

1) Initialize $\eta_{\min}$ and $\eta_{\max}$;
2) **REPEAT**
3) $\eta = (\eta_{\min} + \eta_{\max})/2$;
4) **REPEAT**, Initialize $\mathbf{Q}_1^m(0), \cdots, \mathbf{Q}_K^m(0)$, $n = 1$;
5) **FOR** $k = 1, \cdots, K$
6) $\mathbf{Q}_k^m(n) = [\mathbf{Q}_k^m(n-1) + t\nabla_{\mathbf{Q}_k^m} L]^+$,
7) **END FOR**;
8) $n = n + 1$;
9) **UNTIL** $\mathbf{Q}_K^m$ for $k = 1, \cdots, K$ converge, i.e., $||\nabla_{\mathbf{Q}_k^m} L||^2 \leq \epsilon$ for a small present ϵ.
10) if $\sum_{k=1}^K \mathrm{Tr}(\mathbf{Q}_k^m) > P_T$, $\eta_{\min} = \eta$, elseif $\sum_{k=1}^K \mathrm{Tr}(\mathbf{Q}_k^m) < P_T$, $\eta_{\max} = \eta$;
11) **UNTIL** $|\eta_{\min} - \eta_{\max}| \leq \varepsilon$.

gradient of (46) based on $\mathbf{Q}_k^m$ as follows

$$\nabla_{\mathbf{Q}_k^m} L := \mathbf{I}_{N_r \times N_r} - \eta \frac{\partial f\left[\mathbf{Q}_1^m(n), \cdots, \mathbf{Q}_{k-1}^m(n), \mathbf{Q}_k^m(n-1), \cdots, \mathbf{Q}_K^m(n-1)\right]}{\partial \mathbf{Q}_k^m(n-1)} \tag{52}$$

$$\mathbf{Q}_k^m(n) = \left[\mathbf{Q}_k^m(n-1) - t\nabla_{\mathbf{Q}_k^m} L\right]^+, \tag{53}$$

where t is the step size, and the notation $[\mathbf{D}]^+$ is defined as $[\mathbf{D}]^+ := \sum_i [q_i]^+ \mathbf{v}_i \mathbf{v}_i^H$, where q_i and $\mathbf{v}_i$ are the i^{th} eigenvalue and the corresponding eigenvector of $\mathbf{D}$ respectively. The gradient in (52) can be promptly determined as

$$\frac{\partial f\left(\mathbf{Q}_1^m, \cdots, \mathbf{Q}_K^m\right)}{\partial \mathbf{Q}_k^m} = \mathbf{H}_k \left(\mathbf{I}_{N_t \times N_t} + \frac{1}{\sigma^2} \sum_{k=1}^K \mathbf{H}_k^H \mathbf{Q}_k^m \mathbf{H}_k\right)^{-1} \mathbf{H}_k^H. \tag{54}$$

After the dual MAC covariance matrices $\mathbf{Q}_k^m$ are determined for all users, we need to obtain the optimal η. Due to the convexity property of the Lagrangian function $g(\eta)$, the optimal η can be determined through a one-dimensional search process. However, since $g(\eta)$ is not necessarily differentiable, the gradient algorithm is not suitable in this case. Alternatively, we can apply the subgradient method to find the optimal solution. In each iterative step, η is updated according to the subgradient which is provided as the following lemma.

Lemma I: The subgradient of $g(\eta)$ is $P_T - \sum_{k=1}^K \mathrm{Tr}(\mathbf{Q}_k^m)$, where $\eta > 0$ and $\mathbf{Q}_k^m, k = 1, 2, \cdots, K$, are the corresponding optimal covariance matrices for a fixed η in (50).

Proof: See Appendix D.

Upon convergence of the transmit covariance matrix $\mathbf{Q}_k^m$, we compare the current transmission power in dual MAC with P_T. *Lemma I* indicates that the value of η should increase if $\sum_{k=1}^K \mathrm{Tr}(\mathbf{Q}_k^m) > P_T$, and decrease otherwise. This process will continue until $g(\eta)$ converges.

With the aforementioned theorems and lemma, the dual MAC optimization problem in (43), (44) can now be solved by the proposed bisection based approach, listed in Table II. In Table III, the complexity of the aforementioned SVD-IA and DPC-IA is listed for comparison. The complexity of DPC are based on QR decomposition in [35] while the complexity of grouping-IA is based on [25]. We calculate the computational complexity based on the number of floating points [36]. As can be seen from Table III, the I-ZF scheme proposed in [26] has a higher computational complexity compared to the two proposed schemes.

TABLE III
COMPLEXITY COMPARISON FOR THE PROPOSED ALGORITHMS

Algorithm	Complexity
I-ZF [26]	$\mathcal{O}(K^5(K-1)^2L^4(L-1)^2d_s^6)$
SVD-IA	$\mathcal{O}(K^5(K-1)^2(L-1)^6d_s^6)$
DPC-IA	$\mathcal{O}(K^3(K-1)^4(L-1)^4(L-2)^2d_s^6)$

TABLE IV
LIST OF SIMULATION PARAMETERS

Bandwidth, B	10 MHz
Number of cells, L	3
Number of users at each cell, K	3
Maximum transmit power	46 dBm
Noise power	-110 dBm
Minimum cell throughput requirement	100 Mbps
Drain efficiency of the power amplifier ζ	38%

D. A Complete Solution to the EE Optimization Problem

We are now ready to present a complete algorithm to solve the EE optimization problem in (40)–(42) The transmission power is first initialized as $P_T(0)$, and the maximum EE, $\lambda_{EE}^*(P_T)$, is calculated using the proposed bisection based resource allocation algorithm in Table II. The P_T is updated based on *Theorem III* and utilize the following searching scheme

$$P_T(n) = \begin{cases} \frac{P_T(n-1)}{\beta} & \left.\frac{d\lambda_{EE}^*(P_T)}{dP_T}\right|_{P_T(n-1)} < 0 \\ \beta P_T(n-1) & \text{otherwise} \end{cases}, \tag{55}$$

where $\beta > 1$ is the searching step. Moreover, β needs to be reduced when the gradient $\frac{d\lambda_{EE}^*(P_T)}{dP_T}$ changes sign as in

$$\beta(n) = \frac{\beta(n-1)}{2} \tag{56}$$

and (55) is repeated until convergence, i.e., $|P_T(n+1) - P_T(n)| \leq \epsilon$ or either P_{max} or P_{min} is reached. In other words, the proposed resource allocation algorithm would converge to the optimal point or the boundary point (power constraint). The computational complexity of the outer-layer algorithm depends on the number of iterations and is given by $\mathcal{O}(\frac{1}{\beta^2}\frac{1}{\epsilon^2}N_tK)$.

VI. SIMULATION RESULTS

In this section, we present simulation results to verify the theoretical findings and analyze the effectiveness of the proposed algorithms in terms of EE. We refer to the scheme in Section IV as SVD-IA and the approach in Section V as DPC-IA. All the cells are ordered in an warped around linear array and each BS is surrounded by uniformly-distributed users. The drain efficiency of the power amplifier ζ is set to 38% in our simulation. Signal to noise ratio is defined as $\frac{P_{max}}{\sigma^2}$ and is set to 10 dB. Unless stated otherwise, the power budget for each BS is set to 46 dBm while the minimum cell throughput requirement is set to 100 Mbps. We assume there are three cells with three users in each cell, and BS transmit $d_s = 2$ data streams for each user. Other simulation parameters are shown in Table IV. Simulation results are averaged over 10 000 Monte-Carlo trials.

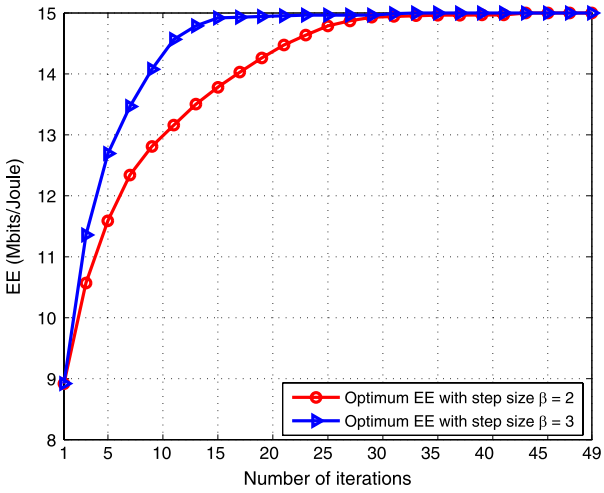

Fig. 2. The convergence behavior of the proposed two-layer resource allocation scheme.

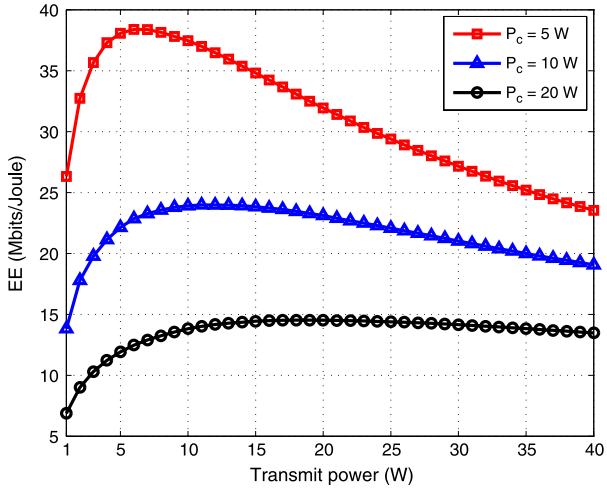

Fig. 4. λ_{EE}^{*}-versus-P_T curves using DPC-IA with different circuit power parameters ($L = 3$, $K = 3$, $d_s = 2$, $\delta_{min} = 100$ Mbps and CNR $= 10$ dB).

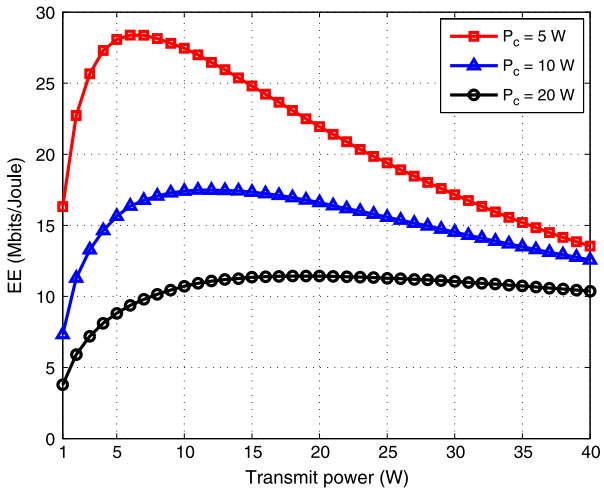

Fig. 3. λ_{EE}^{*}-versus-P_T curves using SVD-IA with different circuit power parameters ($L = 3$, $K = 3$, $d_s = 2$, $\delta_{min} = 100$ Mbps and CNR $= 10$ dB).

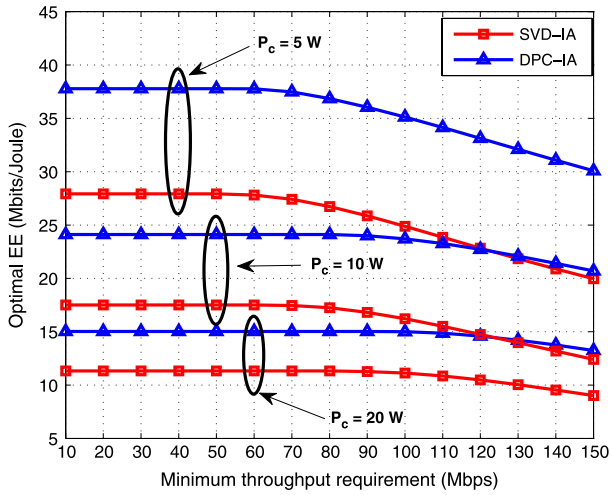

Fig. 5. Maximum EE under different minimum throughput constraints with different circuit power parameters ($L = 3$, $K = 3$, $d_s = 2$, $P_{max} = 46$ dBm and CNR $= 10$ dB).

In the first simulation, the performance of the proposed two layer resource allocation scheme is investigated. The convergence behavior of the proposed approach is first evaluated by illustrating how the EE performance behaves with the number of iterations, and is shown in Fig. 2. As it can be seen from the figure, EE converge after approximately 40 iterations when $\beta = 2$. However, the convergence procedure reduces to 17 iterations when a larger step size is chosen, i.e., $\beta = 3$. This result coincides with our theoretical findings where the computational complexity is inversely proportional to the square of the step size β^2. We then evaluate the EE to transmission power relationship for the case with different total circuit power ($P_c = 5, 10, 20$ W) for both SVD-IA and DPC-IA. It can be seen from Figs. 3 and 4 that the EE-transmission power relationship has a bell shape curve and is quasiconcave. This quasiconcavity is the foundation of the proposed methodology and infers that the proposed water-filling based resource allocation algorithm for SVD-IA always leads to the maximum EE performance. It also implies that the proposed bisection based resource allocation algorithm for DPC-IA can serve as an optimal inner layer step for EE maximization. Figs. 3 and 4 also compare and indicate the influence of circuit power on the EE-transmission power relation. From there, as expected, λ_{EE}^{opt} decreases with increased circuit power due to the higher power consumption. On the other hand, we can observe that the respective P_T^{opt} increases. This is because in this case if the transmission power is small, the total power consumption will be dominated by the circuitry consumption. With the low achievable throughput, the EE will therefore be worse. The optimal EE will occur when the transmission power is comparable to the circuit power consumption, resulting in a higher P_T^{opt}.

In the next simulation, we evaluate the maximum EE under different minimum throughput requirement and different circuit power settings. Fig. 5 presents the maximum EE against different minimum throughput requirements while Fig. 6 shows the corresponding throughput. It can be observed from Fig. 5 that the optimal EE is the same up to a certain minimum throughput requirement, but drops afterwards. This can be explained using the quasiconcavity of EE-transmission power relationship from

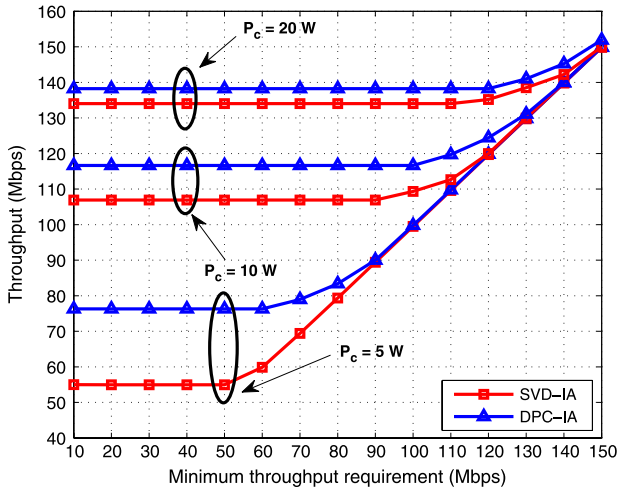

Fig. 6. Corresponding throughput under different minimum throughput constraints with different circuit power parameters ($L = 3$, $K = 3$, $d_s = 2$, $P_{max} =$ 46 dBm and CNR $= 10$ dB).

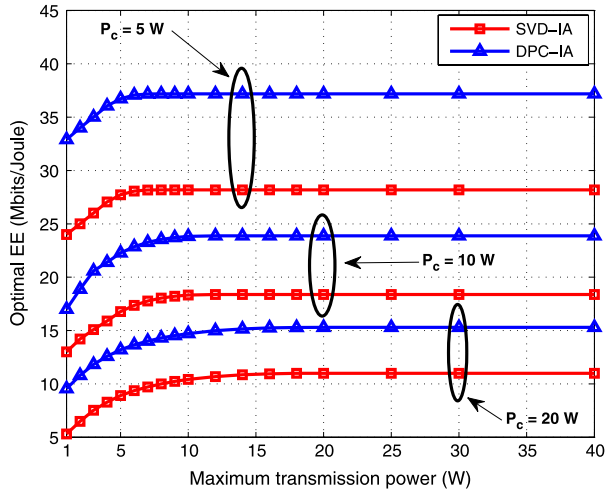

Fig. 7. Maximum EE under different maximum power constraints with different circuit power parameters ($L = 3$, $K = 3$, $d_s = 2$, $\delta_{min} = 100$ Mbps and CNR $= 10$ dB).

Figs. 3 and 4. When the minimum throughput requirement is low, the required transmit power is also low. Therefore, the most energy efficient design is to operate at a higher transmit power in order to achieve the optimal EE. This is why the optimal EE is constant for low minimum throughput requirements and is the same as the optimal EE point from Figs. 2 or 3 correspondingly. For example for DPC-IA with $P_c = 5$ W, the optimal EE from Fig. 3 is 38 Mbps/J, which is the same as that in Fig. 4. However when the minimum throughput requirement is high, the optimal operation is to simply fulfill that throughput requirement as in this case the higher the throughput, the lower the EE. This can also be observed from Fig. 5 as the achievable throughput is exactly the minimum throughput requirement in those regions.

We then evaluate the maximum EE considering different maximum transmission power in the BS. The throughput constraint is restricted to 1 Mbps in order to examine the influence by the maximum allowable transmission power $P_{\max}$. As can be seen from Fig. 7, when the maximum transmission power is smaller than or equal to a certain value, the maximum EE for both SVD-IA and DPC-IA increase with $P_{\max}$. This can again be explained using the results in Figs. 3 and 4 that in low transmit power region, the most energy efficient design is to operate at a higher transmit power. On the contrary, when $P_{\max}$ is high, the optimal operation is to transmit at the power that achieves the maximum EE. In other words, once the optimal EE is reached, further increasing the maximum allowable transmission power will not improve the EE performance. Therefore, network operators will need to ensure a sufficient available transmit power to operate at the most energy efficient manner.

Finally, we compare the maximum EE obtained by the proposed algorithms using SVD-IA and DPC-IA at different SNR operating regimes. To show the EE loss by considering the inter-cell interference in multi-cell scenario, we compare with the optimal EE scheme in single-cell multi-user scenario from [21] (denoted as SC-MU). In other words, SC-MU is the upper bound on EE in multi-cell scenario. We also compare with the interference zero forcing algorithm [26] (denoted as I-ZF) and a greedy scheme such that each cell maximizes its own EE whilst introducing interference to other cells (denoted as Greedy DPC). We first consider the single data stream case ($d_s = 1$) for the BS. As shown in Fig. 8, for a moderate range of SNR, DPC-IA outperforms SVD-IA in terms of EE. However, at high SNR regime, SVD-IA is better; this is because SVD-IA aims to fully utilize the available degrees of freedom for transmission and hence suitable for high SNR regime. On the other hand, pure IA may lead to lower network capacity in low to intermediate SNR region due to the lack of coherent array gain [30]. Hence, DPC-IA scheme which only cancel the inter-cell users and tackle the intra-cell interference among users by designing the beamformers to maximize EE of each cell, is suitable low to intermediate SNR region. Furthermore, as expected, the maximum EE obtained by SC-MU is higher than both SVD-IA and DPC-IA. Nonetheless, DPC-IA achieves an optimal EE that is close to the SC-MU case at low to moderate SNR region, demonstrating the effectiveness of the proposed scheme. This also shows that even though IA generally performs better in high SNR region, the proposed IA schemes can achieve a close-to-optimal EE performance at low to moderate SNR range. On the other hand, comparing the two interference-nulling-based approaches, the maximum EE obtained by SVD-IA outperforms I-ZF over all the SNR region. This is because the proposed SVD-IA approach requires less number of transmit antennas compared to the I-ZF scheme. For instance in the simulation example where $d_s = 1$, we require $N_t = 7$ for the SVD-IA and $N_t = 9$ for the I-ZF, and hence SVD-IA provides diversity gains over the I-ZF scheme. Meanwhile, due to high inter-cell interference, the maximum EE obtained using the Greedy DPC delivers the worst performance out of all the schemes under consideration. These results show that the proposed scheme outperforms all existing approaches in terms of EE optimization. Finally the case of two data stream $d_s = 2$ is evaluated in Fig. 9. It shows a similar trend for all the solutions as in Fig. 8. However, the intersection point between DPC-IA and SVD-IA is increased (from 15 dB in Fig. 8 to 19 dB in Fig. 9). This reveals that the proposed DPC-IA is superior to the proposed SVD-IA when multiple data streams are transmitted.

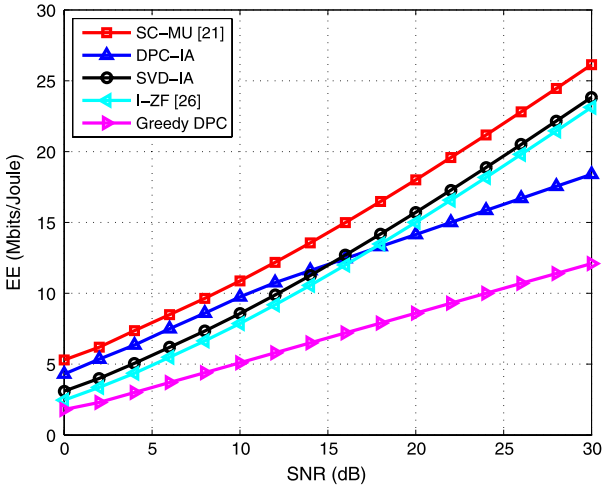

Fig. 8. Maximum EE for SVD-IA and DPC-IA with different number of antennas setting ($L=3$, $K=3$, $d_s=1$, $\delta_{min}=100$ Mbps and $P_{max}=46$ dBm).

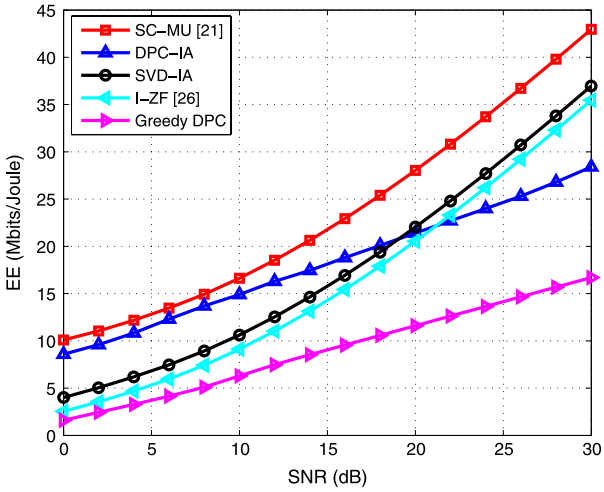

Fig. 9. Maximum EE for SVD-IA and DPC-IA with different number of antennas setting ($L=3$, $K=3$, $d_s=2$, $\delta_{min}=100$ Mbps and $P_{max}=46$ dBm).

VII. Conclusion

In this paper, we addressed the EE optimization problem for multi-cell MIMO-IFBC with IA. We proposed two schemes to optimize EE for different SNR regions. For high SNR region, we employ a grouping-based IA scheme to cancel inter- and intra-cell interference and transform the MIMO-IFBC to a single-cell single user MIMO scenario. A gradient-based power adaptation scheme has been proposed based on the water-filling approach and SVD to maximize EE for each cell. For a moderate range of SNR, we propose a method using DPC and MAC-BC duality to perform IA while maximizing EE in each cell. Accordingly, a novel inner-layer algorithm was proposed by applying the principle of MAC-BC duality. Simulation results demonstrate that the proposed schemes outperform several existing approaches in all SNR range. More importantly, the proposed DPC-IA scheme achieves an optimal EE that is close to the single cell scenario at low to medium SNR range, which is normally the energy efficient operating region.

Appendix A
Proof of Theorem I

Proof: With the nature of water-filling, it is easy to prove that the transmit power on each data stream is nondecreasing with the total transmit power. We here consider the limit under the constraint $\sum_{k\in\mathcal{K}}\sum_{i\in\mathcal{S}_i}\triangle p_{[k,i]}=\triangle P_T$. The existence of the limit indicates that $\tilde{R}(P_T)$ is continuously differentiable in P_T and

$$\frac{d\tilde{R}(P_T)}{dP_T}=\frac{d\tilde{R}(P_T)}{dp_{[k,i]}}=\max_{k\in\mathcal{K},i\in\mathcal{S}_i}\frac{Wg_{[k,i]}\log_2 e}{1+\tilde{p}_{[k,i]}g_{[k,i]}}. \tag{57}$$

Moreover, $\frac{Wg_{[k,i]}\log_2 e}{1+\tilde{p}_{[k,i]}g_{[k,i]}}$ is nonincreasing with P_T for $k\in\mathcal{K}$ and $i\in\mathcal{S}_i$ while $\max_{k\in\mathcal{K},i\in\mathcal{S}_i}\frac{Wg_{[k,i]}\log_2 e}{1+\tilde{p}_{[k,i]}g_{[k,i]}}$ is strictly monotonically decreasing with P_T. Thus, $\frac{d^2\tilde{R}(P_T)}{dP_T^2}<0$ and $\tilde{R}(P_T)$ is strictly concave in P_T.

In order to prove the quasiconcavity of $\tilde{\lambda}_{EE}(P_T)$, we first introduce definition of quasiconcave function. According to [37], a function $f:\mathbf{R}^n-\mathbf{R}$ is called quasiconvex if its domain and all its sublevel sets

$$\mathcal{S}_\theta=\{x\in\mathbf{dom}f|f(x)\le\theta\}, \tag{58}$$

for $\theta\in\mathbf{R}$, are convex. A function is quasiconcave if $-f$ is quasiconvex, i.e., every superlevel set $x|f(x)\ge\theta$ is convex. Hence, $\frac{\tilde{R}(P_T)}{P}$ is strictly quasiconcave in P_T if $\mathcal{S}_\theta$ is strictly convex for any real number θ. When $\theta<0$, no points exist on the counter $\frac{\tilde{R}(P_T)}{P}=\theta$. When $\theta\ge 0$, $\mathcal{S}_\theta$ is equivalent to $\mathcal{S}_\theta=\{P_T\ge P_0|\theta\zeta P_T+\theta P_C-\tilde{R}(P_T)\}\le 0$, where P_0 is the minimum transmit power for realizing minimum throughput $\delta_{\min}$. Since $\tilde{R}(P_T)$ is strictly concave in P_T, $\mathcal{S}_\theta$ is strictly convex in P_T. Therefore, $\frac{\tilde{R}(P_T)}{P}$ is continuously differentiable and quasiconcave in P_T and this completes the proof of Property (i) of *Theorem I*.

Furthermore, we analysis $\frac{d\frac{\tilde{R}(P_T)}{P}}{dP_T}$ as follows

$$\begin{aligned}\frac{d\frac{\tilde{R}(P_T)}{P}}{dP_T}&=\lim_{\triangle P_T\to 0}\frac{\frac{\tilde{R}(P_T+\triangle P_T)}{\zeta(P_T+\triangle P_T)+P_C}-\frac{\tilde{R}(P_T)}{\zeta P_T+P_C}}{\triangle P_T}\\&=\lim_{\triangle P_T\to 0}\frac{\frac{\tilde{R}(P_T+\triangle P_T)-\tilde{R}(P_T)}{\triangle P_T}-\zeta\tilde{\lambda}_{EE}(P_T)}{\zeta(P_T+\triangle P_T)+P_C}\\&=\frac{\frac{d\tilde{R}(P_T)}{dP_T}-\zeta\tilde{\lambda}_{EE}(P_T)}{\zeta P_T+P_C}.\end{aligned} \tag{59}$$

This completes the proof of Property (ii) of *Theorem I*. □

Appendix B
Proof of Theorem II

Proof: Similar as the proof of *Theorem I*, we denote the superlevel sets of $\lambda^*_{EE}(P_T)$ as

$$\mathcal{S}_\nu=\left\{P_T\ge P_{min}|\lambda^*_{EE}(P_T)\ge\nu\right\}. \tag{60}$$

According to [37], $\lambda^*_{EE}(P_T)$ is strictly quasiconcave in P_T if $\mathcal{S}_\nu$ is strictly convex for any real number ν. When $\nu<0$, no

points exist on the counter $\lambda^*_{EE}(P_T) = \theta$. When $\nu \geq 0$, λ_{EE} is written as $\lambda_{EE} = \frac{C_{MAC}}{\zeta P_T + P_c}$, hence $\mathcal{S}_\nu = \{P_T \geq P_{min} | \beta\zeta P_T + \beta P_C - C_{MAC}(P_T)\} \leq 0$, Since $C_{MAC}(P_T)$ is strictly concave in P_T, $\mathcal{S}_\nu$ is strictly convex in P_T. Therefore, the maximum EE is strictly quasiconcave in P_T and this completes the proof of *Theorem II*. □

Appendix C
Proof of Theorem III

Proof: In order to prove *Theorem III*, we analyze the limit of $\lambda^*_{EE}(P_T)$ as follows

$$\begin{aligned}\lim_{P_T\to\infty} \lambda^*_{EE}(P_T) &= \lim_{P_T\to\infty} \max_{\mathbf{Q}^b_k \succeq 0} \frac{C_{MAC}(P_T)}{\zeta P_T + P_c} \\ &= \lim_{P_T\to\infty} \frac{o(P_T)}{\zeta P_T + P_c} \\ &= 0. \end{aligned} \tag{61}$$

Hence, with strict concavity of $\lambda^*_{EE}(P_T)$ which is proved in Appendix B, starting from $P_T = P_{min}$, $\lambda^*_{EE}(P_T)$ either strictly decreases with P_T if $\frac{d\lambda^*_{EE}(P_T)}{dP_T}\Big|_{P_T=P_{min}} \leq 0$, or first strictly increases and then strictly decreases with P_T if $\frac{d\lambda^*_{EE}(P_T)}{dP_T}\Big|_{P_T=P_{min}} > 0$, and the maximum EE in the power region $[P_{min}, P_{max}]$ is straightforward as indicated in *Theorem III*. This completes the proof. □

Appendix D
Proof of Lemma I

Proof: Let ν be the subgradient of $g(\check{\eta})$. For a given $\check{\eta} > 0$, the subgradient ν of $g(\check{\eta})$ satisfies $g(\hat{\eta}) \geq g(\check{\eta}) + \nu(\hat{\eta} - \check{\eta})$, where $\hat{\eta}$ is any feasible value. Let $\hat{\mathbf{Q}}^m_k, \{k = 1, \cdots, K\}$, denote the optimal covariance matrices in (50) for $\eta = \hat{\eta}$, and $\check{\mathbf{Q}}^m_k, \{k = 1, \cdots, K\}$, denote the optimal covariance matrices in (50) for $\eta = \check{\eta}$. We express $g(\hat{\eta})$ as

$$\begin{aligned} g(\hat{\eta}) &= \max_{\mathbf{Q}^m_k \succeq 0} f\left(\mathbf{Q}^m_1, \cdots, \mathbf{Q}^m_K\right) - \hat{\eta}\left[\sum_{k=1}^K tr\left(\mathbf{Q}^m_k\right) - P_T\right] \\ &= f\left(\hat{\mathbf{Q}}^m_1, \cdots, \hat{\mathbf{Q}}^m_K\right) - \hat{\eta}\left[\sum_{k=1}^K tr\left(\hat{\mathbf{Q}}^m_k\right) - P_T\right] \\ &\geq f\left(\check{\mathbf{Q}}^m_1, \cdots, \check{\mathbf{Q}}^m_K\right) - \hat{\eta}\left[\sum_{k=1}^K tr\left(\check{\mathbf{Q}}^m_k\right) - P_T\right] \\ &= f\left(\check{\mathbf{Q}}^m_1, \cdots, \check{\mathbf{Q}}^m_K\right) - \check{\eta}\left[\sum_{k=1}^K tr\left(\check{\mathbf{Q}}^m_k\right) - P_T\right] \\ &\quad + \check{\eta}\left[\sum_{k=1}^K tr\left(\check{\mathbf{Q}}^m_k\right) - P_T\right] - \hat{\eta}\left[\sum_{k=1}^K tr\left(\check{\mathbf{Q}}^m_k\right) - P_T\right] \\ &= g(\check{\eta}) + (\hat{\eta} - \check{\eta})\left[P_T - \sum_{k=1}^K tr\left(\check{\mathbf{Q}}^m_k\right)\right] \end{aligned} \tag{62}$$

where $\nu := P_T - \sum_{k=1}^K tr(\check{\mathbf{Q}}^m_k)$ is the subgradient of $g(\check{\eta})$. This concludes the proof. □

References

[1] M. Kang, M. S. Alouini, and L. Yang, "Outage probability and spectrum efficiency of cellular mobile radio systems with smart antennas," *IEEE Trans. Commun.*, vol. 50, no. 7, pp. 1871–1877, Dec. 2002.

[2] H. Dai and H. Poor, "Asymptotic spectral efficiency of multi-cell MIMO systems with frequency-flat fading," *IEEE Trans. Signal Process.*, vol. 51, no. 11, pp. 2976–2988, Nov. 2003.

[3] S. Verdu, "Spectral efficiency in the wideband regime," *IEEE Trans. Inf. Theory*, vol. 48, no. 6, pp. 1319–1343, Jun. 2002.

[4] R. S. Prabhu and B. Daneshrad, "Energy-efficient power loading for a MIMO-SVD system and its performance in flat fading," in *Proc. IEEE Globecom*, Dec. 2010, pp. 1–5.

[5] R. S. Prabhu and B. Daneshrad, "Performance analysis of energy-efficient power allocation for MIMO-MRC systems," *IEEE Trans. Commun.*, vol. 60, no. 8, pp. 2048–2053, Aug. 2012.

[6] C. Hellings, N. Damak, and W. Utschick, "Energy-efficient zero-forcing with user selection in parallel vector broadcast channels," in *Proc. Int. ITG WSA*, Mar. 2012, pp. 168–175.

[7] C. Xiong, G. Li, S. Zhang, Y. Chen, and S. Xu, "Energy-efficient resource allocation in OFDMA networks," *IEEE Trans. Commun.*, vol. 60, no. 12, pp. 3767–3778, Dec. 2012.

[8] G. Miao, N. Himayat, and G. Y. Li, "Energy-efficient link adaptation in frequency-selective channels," *IEEE Trans. Commun.*, vol. 58, no. 2, pp. 545–554, Feb. 2010.

[9] G. Koutitas, A. Karousos, and L. Tassiulas, "Deployment strategies and energy efficiency of cellular networks," *IEEE Trans. Wireless Commun.*, vol. 11, no. 7, pp. 2552–2563, Jul. 2012.

[10] S. He, Y. Huang, S. Jin, and L. Yang, "Coordinated beamforming for energy efficiency maximization in multi-cell multiuser systems," *IEEE Trans. Commun.*, vol. 61, no. 12, pp. 4961–4971, Dec. 2013.

[11] C. Ghosh and S. Roy, "Coexistence challenges for heterogeneous cognitive wireless networks in TV white spaces," *IEEE Wireless Commun.*, vol. 18, no. 4, pp. 22–31, Aug. 2011.

[12] J. Mao, G. Xie, J. Gao, and Y. Liu, "Energy efficiency optimization for OFDM-based cognitive radio systems: A waterfilling factor aided search method," *IEEE Trans. Wireless Commun.*, vol. 12, no. 5, pp. 2366–2375, May 2013.

[13] Z. Hasan, H. Boostanimehr, and V. K. Bhargava, "Green cellular networks: A survey, some research issues and challenges," *IEEE Commun. Surveys Tuts.*, vol. 13, no. 4, pp. 524–540, 4th Quart. 2011.

[14] D. Gesbert, M. Kountouris, R. Heath, C.-B. Chae, and T. Salzer, "Shifting the MIMO paradigm," *IEEE Signal Process. Mag.*, vol. 24, no. 5, pp. 36–46, Sep. 2007.

[15] G. J. Foschini and M. J. Gans, "On limits of wireless communications in a fading environment when using multiple antennas," *Wireless Pers. Commun.*, vol. 6, pp. 311–335, 1998.

[16] H. Weingarten, Y. Steinberg, and S. Shamai, "The capacity region of the Gaussian multiple-input multiple-output broadcast channel," *IEEE Trans. Inf. Theory*, vol. 52, no. 9, pp. 3936–3964, Sep. 2006.

[17] G. Caire and S. Shamai, "On the achievable throughput of a multiantenna Gaussian broadcast channel," *IEEE Trans. Inf. Theory*, vol. 49, no. 7, pp. 1691–1706, Jul. 2003.

[18] J. Tang, D. K. C. So, E. Alsusa, and K. A. Hamdi, "Resource efficiency: A new paradigm on energy efficiency and spectral efficiency tradeoff," *IEEE Trans. Wireless Commun.*, vol. 13, no. 8, pp. 4656–4669, Aug. 2014.

[19] Z. Chong and E. Jorswieck, "Energy efficiency in random opportunistic beamforming," in *Proc. Veh. Technol. Conf.*, 2011, pp. 1–5.

[20] C. Hellings and W. Utschick, "Energy efficiency optimization in MIMO broadcast channels with fairness constraints," in *Proc. 14th Int. Workshop Signal Process. Adv. Wireless Commun.*, Darmstadt, Germany, Jun. 2013, pp. 599–603.

[21] J. Xu and L. Qiu, "Energy efficiency optimization for MIMO broadcast channels," *IEEE Trans. Wireless Commun.*, vol. 12, no. 2, pp. 690–701, Feb. 2013.

[22] W. Rao and L. Dai, "On capacity bounds of multi-cell MIMO broadcast channel," in *Proc. ICISE*, Dec. 2009, 26–28.

[23] H. D. Nguyen, R. Zhang, and HonTatHu, "multi-cell random beamforming: Achievable rate and degrees of freedom region," *IEEE Trans. Signal Process.*, vol. 61, no. 14, pp. 3532–3544, Jul. 2013.

[24] S. H. Park and I. Lee, "Degrees of freedom and sum rate maximization for two mutually interfering broadcast channels," in *Proc. IEEE ICC*, Dresden, Germany, Jun. 2009, pp. 1–5.

[25] J. Tang and S. Lambotharan, "Interference alignment techniques for MIMO multi-cell interfering broadcast channels," *IEEE Trans. Commun.*, vol. 61, no. 1, pp. 164–175, Jan. 2013.

[26] J. Zhang, X. Wang, and W. Li, "Energy efficiency of partial-cooperative multi-cell system based on interference zero-forcing," in *Proc. Int. Conf. WCSP*, Hangzhou, China, Oct. 2013, pp. 1–4.

[27] G. Miao, N. Himayat, G. Y. Li, and A. Swami, "Cross-layer optimization for energy-efficient wireless communications: A survey," *Wiley J. Wireless Commun. Mobile Comput.*, vol. 9, no. 4, pp. 529–542, Apr. 2009.
[28] S. Cui, A. Goldsmith, and A. Bahai, "Energy-constrained modulation optimization," *IEEE Trans. Wireless Commun.*, vol. 4, no. 5, pp. 2349–2360, Sep. 2005.
[29] E. Bjornson, L. Sanguinetti, J. Hoydis, and M. Debbah, "Optimal design of energy-efficient multi-user MIMO systems: Is massive MIMO the answer?" *IEEE Trans. Wireless Commun.*, vol. 14, no. 6, pp. 3059–3075, Jun. 2015.
[30] K. Gomadam, V. R. Cadambe, and S. A. Jafar, "A distributed numerical approach to interference alignment and applications to wireless interference networks," *IEEE Trans. Inf. Theory*, vol. 57, no. 6, pp. 3309–3322, Jun. 2011.
[31] S. Vishwanath, N. Jindal, and A. Goldsmith, "Duality, achievable rates, and sum-rate capacity of Gaussian MIMO broadcast channels," *IEEE Trans. Inf. Theory*, vol. 49, no. 10, pp. 2658–2668, Oct. 2003.
[32] W. Dinkelbach, "On nonlinear fractional programming," *Manage. Sci.*, vol. 13, no. 7, pp. 492–498, Mar. 1967.
[33] M. Avriel, W. E. Diewert, S. Schaible, and I. Zang, *Generalized Concavity*. New York, NY, USA: Plenum, 1988.
[34] K. T. K. Cheung, S. Yang, and L. Hanzo, "Achieving maximum energy-efficiency in multi-relay OFDMA cellular networks: A fractional programming approach," *IEEE Trans. Commun.*, vol. 61, no. 7, pp. 2746–2757, Jul. 2013.
[35] L.-N. Tran, M. Juntti, M. Bengtsson, and B. Ottersten, "Weighted sum rate maximization for MIMO broadcast channels using dirty paper coding and zero-forcing methods," *IEEE Trans. Commun.*, vol. 61, no. 6, pp. 2362–2373, Jun. 2013.
[36] M. P. Holmes, A. G. Gray, and C. L. Isbell, "Fast SVD for large-scale matrices," College Comput., Georgia Instit. Technol., Atlanta, GA, USA.
[37] S. Boyd and L. Vandenberghe, *Convex Optimization*. Cambridge, U.K.: Cambridge Univ. Press, 2004.

Jie Tang (S'10–M'13) received the B.Eng. degree in information engineering from South China University of Technology, Guangzhou, China, in 2008, the M.Sc. degree (with distinction) in communication systems and signal processing from the University of Bristol, Bristol, U.K., in 2009, and the Ph.D. degree from Loughborough University, Loughborough, U.K., in 2012. Since 2013, he has been a Postdoctoral Research Associate with the School of Electrical and Electronic Engineering, The University of Manchester, Manchester, U.K. His research interests include optimization techniques and analysis of wireless communication networks, with particular focus on green communications, 5G systems, heterogeneous networks, cognitive radio, MIMO systems, and cooperative MIMO schemes.

Daniel K. C. So (S'96–M'03–SM'14) received the B.Eng. degree (with first-class honor) in electrical and electronics engineering from The University of Auckland, Auckland, New Zealand, in 1996 and the Ph.D. degree in electrical and electronics engineering from Hong Kong University of Science and Technology, Hong Kong, in 2003. From 1997 to 1998, he was with Orion Systems International Ltd., Auckland, where he was initially a Software Engineer and was later promoted to a Senior Software Engineer. Since 2003, he has been with The University of Manchester, Manchester, U.K., where he was a Lecturer and is currently a Senior Lecturer in the School of Electrical and Electronic Engineering. He has been also serving as the Director of Postgraduate Taught since 2009 at The University of Manchester. His research interests include green communications, 5G network, heterogeneous networks, cognitive radio, massive MIMO, D2D communications, cooperative MIMO, multihop communication, OFDM, single-carrier FDMA, multicarrier CDMA, and channel equalization and estimation techniques. Dr. So regularly serves on the technical program committee of major international conferences and is a Track Cochair for VTC Spring 2016.

Emad Alsusa (M'06–SM'07) received the Ph.D. degree in electrical and electronic engineering from the University of Bath, Bath, U.K., in 2000. He then joined The University of Edinburgh, as a Mobile VCE Postdoctoral Research Fellow, working on link enhancement techniques for future high-data-rate wireless communication systems. In 2003, he joined The University of Manchester, Manchester, U.K., as an Academic Member of the School of Electrical and Electronic Engineering, where he lectures on communication engineering subjects. His research interests include signal processing techniques and analysis of wireless communication networks, with particular focus on cognitive radio, interference mitigation, multiuser MIMO, GreenComm, and energy and spectrum optimization techniques. Dr. Alsusa served as a Technical Program Committee Member for numerous IEEE flagship conferences and chaired the Manchester EEE Postgraduate Conference in 2010.

Khairi Ashour Hamdi (M'99–SM'02) received the B.Sc. degree in electrical engineering from Al Fateh University, Tripoli, Libya, in 1981, the M.Sc. degree (with distinction) from the Technical University of Budapest, Budapest, Hungary, in 1988, and the Ph.D. degree in telecommunication engineering awarded by the Hungarian Academy of Sciences, Budapest, in 1993. He is currently with the School of Electrical and Electronic Engineering, The University of Manchester, Manchester, U.K. His current research interests include modeling and performance analysis of wireless communication systems and networks.

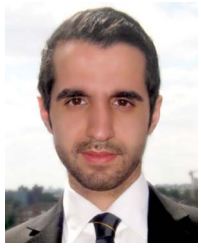

Arman Shojaeifard (S'10–M'13) received the B.Eng. degree in information systems engineering from Imperial College London, London, U.K., in October 2009 and the M.Sc. degree (with distinction) in signal processing for communications and the Ph.D. degree in telecommunications from King's College London, London, in August 2008 and February 2013, respectively. He then worked as a Postdoctoral Research Assistant with the Centre for Telecommunications Research, Department of Informatics, King's College London. Since October 2013, he has been a Postdoctoral Research Associate with the Microwave and Communication Systems research group, School of Electrical and Electronic Engineering, The University of Manchester, Manchester, U.K. His current research interest is in the area of wireless communications theory, with particular focus on the design, modeling, and performance analysis of heterogeneous cellular networks.